

Force spectrum of a few chains grafted on an AFM tip: Comparison of the experiment to a self-consistent mean field theory simulation

Tao Wang, Jiajing Xu, Feng Qiu*, Hongdong Zhang, Yuliang Yang

The Key Lab of Molecular Engineering of Polymers, Ministry of Education of China, Department of Macromolecular Science, Fudan University, Shanghai 200433, China

Received 2 February 2007; received in revised form 15 June 2007; accepted 29 July 2007

Available online 2 August 2007

Abstract

A simulation model based on self-consistent mean field theory (SCMFT) has been developed to inspect the approaching process of the polymer chain grafted AFM tip to a substrate. The effects of various controlling parameters, such as grafting position, chain number, chain length, as well as solvent- and substrate-chain interactions, on the force curve were investigated. Real force spectroscopy of AFM tips modified by poly(ethylene glycol) (PEG) chains interacting with the fresh mica has been recorded, and several typical types of the force curves that correspond to the different states of the grafting chain were assorted. The simulations fit the experimental results well, providing a strong support to the model. © 2007 Elsevier Ltd. All rights reserved.

Keywords: Atomic force microscopy; Self-consistent mean field theory; Force curve

1. Introduction

Atomic force microscope (AFM), a powerful tool for exploring the microscopic and submicroscopic world, has been fast developed since it was invented 20 years ago [1–4]. AFM is widely used not only for morphological observation but also for the evaluation technique of various surface properties, viscoelasticity, friction, crystallization, and so on [5–7]. In the past decade, many researches have focused on the survey of micro-forces ranging from pico- to nano-Newton by using AFM. Examples include the adsorption of molecules onto interfaces [8], estimation of the covalent bond strength [9], conversion of macromolecular configurations [10], measurement of interactions between host and guest molecules [11], and the mechanics of single chains [12], etc. Polymer chains are often required to be grafted onto the tips in many of the above experiments, such as estimating the interaction between antibody and antigen [13], studying the driving force

of self-assembly, etc. Thus it is very essential to develop a useful method to inspect the state of the grafted chains in order to improve the understanding of AFM force spectroscopy. Empirical criteria for single chain stretching, which was based on observing the “cleanness” and normalization of the force curves, the consistency of the molecular parameters fitted from these force curves, as well as the approaching and retracting traces, has been established [14]. Although the knowledge of the chains on the tip is important for further researches, experimental works generally focus on the mechanism of grafting the chains but not on the morphologies and the positions [12]. Some related simulation works have been done by Patra and Linse to discuss the grafted polymers on nanopatterned surface [15], but not on the AFM tip yet.

In polymer physics, self-consistent mean field theory (SCMFT) is among the most accurate and systematic theories at the mean field level [16–18] and it has been widely used in the polymer condensed matter research, such as phase diagram calculating [19], searching for new phases [20], mechanical properties [21], etc. Free of any additional assumptions except the saddle point approximation, SCMFT takes the architectures of macromolecular chains into account conveniently,

* Corresponding author. Tel.: +86 021 5566 4036; fax: +86 021 6564 0293.
E-mail address: fengqiu@fudan.edu.cn (F. Qiu).

therefore providing the information about the macromolecular conformations, the space distribution of the chain segments and the thermodynamics of the system with self-contained mathematical descriptions [22,23]. Here we present an application of SCMFT on the force analysis of the approaching process of the tips with polymer chains grafted. The effects of the grafting position, numbers and lengths of the grafted chains, the solvents and the interaction between the chain segments and the substrate are investigated. Further, different force curves are obtained from the simulation as well. Real force curves from experiments, which lend a strong support to the simulation data, are also presented in this paper. The agreement between the theoretical and the experimental results also gives us much detailed information about the force process, demonstrating a novel method to detect the conditions of the grafted chains. Thermodynamic state of the system is ensured under the measuring conditions.

2. Theory and model

Self-consistent mean field theory (SCMFT) has been used to simulate the process of a polymer chain-grafted tip approaching a substrate. The free energy and the space distribution of the chain segments at various distances between the tip and the substrate have been calculated. By differentiating the free energy with respect to the distance, the force curves are obtained, which can be compared with the result measured from the AFM force experiments.

The system we considered is composed of n_p Gaussian chain(s) with a chain length N and n_s solvent molecules. Assuming the system is incompressible, the volume of the whole system is: $V = Nn_p\rho_0^{-1} + n_s\nu_s$. Here ρ_0^{-1} is the volume of one chain segment (usually the value is set to be 1) and ν_s is the volume of one solvent molecule. The size of a chain segment is b and the relation between ρ_0 and b is $\rho_0 \propto b^{-3}$. Thus the volume ratio of a solvent molecule to that of a chain is $\gamma = \nu_s\rho_0/N$. In SCMFT, external auxiliary fields are used to replace the molecular interactions. When there is no interaction between the chain segments and the substrate, Eqs. (1a) and (1b) are satisfied:

$$w_p(\mathbf{r}) = \xi(\mathbf{r}) + \chi_{ps}\phi_s(\mathbf{r}) \quad (1a)$$

$$w_s(\mathbf{r}) = \xi(\mathbf{r}) + \chi_{ps}\phi_p(\mathbf{r}) \quad (1b)$$

Here χ_{ps} is the interaction parameter between the polymer chain segment and the solvent. $\xi(\mathbf{r})$ is the Lagrange multiplier which ensures the incompressibility of the system, and it can be obtained by Eq. (2) in the simulation as:

$$\xi(\mathbf{r}) = \xi_0 [1 - \phi_p(\mathbf{r}) - \phi_s(\mathbf{r})] \quad (2)$$

where ξ_0 is a constant, and its value should be big enough to make Eq. (3) tenable and the resulting density profiles and free energy should be independent of its particular value. The incompressibility of the system requires:

$$\phi_p(\mathbf{r}) + \phi_s(\mathbf{r}) = 1 \quad (3)$$

In our system, the polymer chain is modeled as a Gaussian chain which is described by a continuous curve $\mathbf{R}(s)$. The variable s increases continuously along the counter length of the chain. Normally, we set the grafted end of the polymer as $s = 0$ and the free end as $s = 1$. Thus a local partition function $q(\mathbf{r}, s)$ of the chain is defined as the summation of the states of the chain segment s at position \mathbf{r} . And $q(\mathbf{r}, s)$ obeys the modified diffusion equation.

$$\frac{\partial}{\partial s} q(\mathbf{r}, s) = \frac{Nb^2}{6} \nabla^2 q(\mathbf{r}, s) - w_p(\mathbf{r}) q(\mathbf{r}, s) \quad (4)$$

Here the initial condition is $q(\mathbf{r}, 0) = \delta(\mathbf{r} - \mathbf{r}_g)$ and \mathbf{r}_g is the position of the grafted point. Since two ends of the grafted chains are different, another local partition function $q^\dagger(\mathbf{r}, s)$ is needed. It obeys the diffusion equation (4) with -1 multiplied on the right side, and the initial condition is $q^\dagger(\mathbf{r}, s) = 1$. Therefore the total partition function of the whole chain is obtained as:

$$Q_p = \int d\mathbf{r} q(\mathbf{r}, s) q^\dagger(\mathbf{r}, s) \quad (5)$$

Likewise, treating them as simple particles, the partition function of the solvent molecules should be written as:

$$Q_s = \int d\mathbf{r} \exp[-\gamma w_s(\mathbf{r})] \quad (6)$$

And thus the local volume fractions of the chain and the solvent could be expressed in Eq. (7), respectively, as:

$$\phi_p(\mathbf{r}) = \frac{\bar{\phi}_p V}{Q_p} \int_0^1 ds q(\mathbf{r}, s) q^\dagger(\mathbf{r}, s) \quad (7a)$$

$$\phi_s(\mathbf{r}) = \exp[-\gamma w_s(\mathbf{r})] \quad (7b)$$

where $\bar{\phi}_p$ is the average volume fraction of the polymers. Similar to all the mean field theories, the auxiliary fields should be self-adjusted to make the local volume fractions of the chain segments and the solvent satisfy Eq. (3).

The free energy of the system can be written as:

$$\begin{aligned} \frac{F}{k_B T \rho_0} = & -\frac{n_p}{\rho_0} \ln\left(\frac{Q_p}{V}\right) - \frac{n_s \gamma}{\rho_0} \ln\left(\frac{Q_s}{V}\right) + \int d\mathbf{r} [\chi_{ps} \phi_p(\mathbf{r}) \phi_s(\mathbf{r}) \\ & - w_p(\mathbf{r}) \phi_p(\mathbf{r}) - w_s(\mathbf{r}) \phi_s(\mathbf{r}) - \xi(\mathbf{r}) (1 - \phi_p(\mathbf{r}) - \phi_s(\mathbf{r}))] \end{aligned} \quad (8)$$

According to Eq. (1), it can be simplified to:

$$\begin{aligned} \frac{F}{k_B T \rho_0} = & -\frac{n_p}{\rho_0} \ln\left(\frac{Q_p}{V}\right) - \frac{n_s \gamma}{\rho_0} \ln\left(\frac{Q_s}{V}\right) - \int \xi(\mathbf{r}) d\mathbf{r} \\ & - \int \chi_{ps} \phi_p(\mathbf{r}) \phi_s(\mathbf{r}) d\mathbf{r} \end{aligned} \quad (9)$$

In order to inspect the influence of the interaction between the chain segments and the substrate, we defined $\eta(\mathbf{r})$ as an interaction parameter between them. The interaction is attractive

when $\eta(\mathbf{r})$ is negative and is repulsive otherwise. Therefore the free energy of the system turns into:

$$\frac{F}{k_B T \rho_0} = -\frac{n_p}{\rho_0} \ln\left(\frac{Q_p}{V}\right) - \frac{n_s \gamma}{\rho_0} \ln\left(\frac{Q_s}{V}\right) - \int \xi(\mathbf{r}) d\mathbf{r} - \int \chi_{ps} \phi_p(\mathbf{r}) \phi_s(\mathbf{r}) d\mathbf{r} + \int \phi_p(\mathbf{r}) \eta(\mathbf{r}) d\mathbf{r} \quad (10)$$

And the corresponding external auxiliary fields are:

$$w_p(\mathbf{r}) = \xi(\mathbf{r}) + \chi_{ps} \phi_s + \eta(\mathbf{r}) \quad (11a)$$

$$w_s(\mathbf{r}) = \xi(\mathbf{r}) + \chi_{ps} \phi_p \quad (11b)$$

where

$$\eta(\mathbf{r}) = \begin{cases} \text{constant} & \text{on the substrate} \\ 0 & \text{other place} \end{cases} \quad (12)$$

By differentiating the free energy with respect to the distance, we can obtain the force curve from the energy–distance curve. We note that in the present form of SCMFT a polymer chain is treated in a coarse-grained level, in which detailed structures such as possible knots in a chain and entanglements between chains are not considered. It has been pointed out that the knotted chains may have observable effect on the force curve in the chain stretching experiment [24]. However, in this paper we focus on the tip-approaching-substrate process, in which the chain is compressed, we expect the excluded volume effect and entropy change are more important than knots formation.

Usually, there are only a few PEG chains grafted onto the AFM tip in the experiment. So we use a simplified model in which only one chain is grafted onto the tip to discuss the general situations (Fig. 1). In the simulation, the size of the chain segment is fixed to b , corresponding to a Kuhn length. Since the system has rotational symmetry about the axis of the tip when the chains are grafted on the top center of the tip, the simulation can be carried out in a (three dimensional) cylindrical coordinate, with a radius of $100b$ and a height of $200b$. Because all the variables have no azimuthal dependence, we solved the SCMFT equations in a coordinate ($r; z$), the details can be found in Ref. [25]. According to the freely jointed chain model, one segment in the simulation represents 2.3 PEG chain segments, thus the lattice unit b is approximately 0.8 nm. The tip size and shape are set to be similar to the real contact tip, with curvature radius being $30b$ (24 nm) and the tip cone angle being 70° . The chain lengths used in simulation are from 20 to 80 segments (with counter lengths 16–64 nm, similar to the lengths of PEG chains with molecular weight ranging from 2000 g/mol to 8000 g/mol).

3. Experiment

3.1. Materials

Methyl poly (ethylene glycol) (MPEG, $M_n = 5000$ g/mol, $D_p = 1.10$) was purchased from Aldrich Corporation and

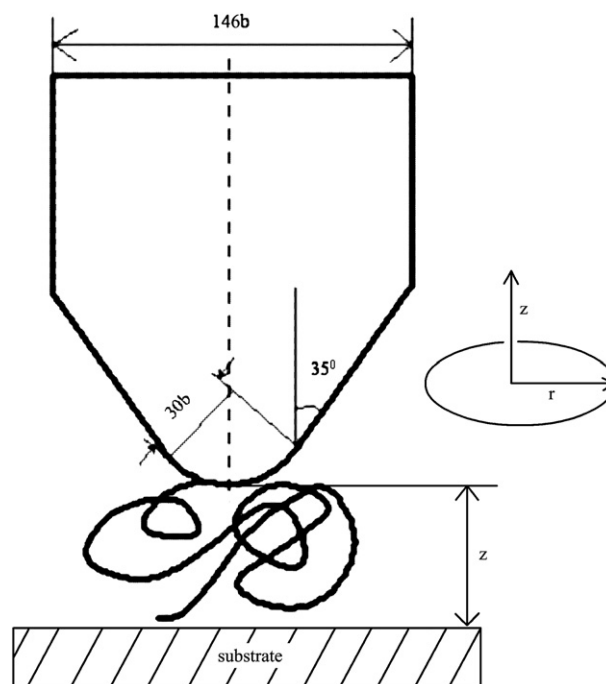


Fig. 1. Model of the polymer chain grafted tip.

used after dried at 50°C in vacuum for more than 24 h. *N*-Hydroxysuccinimide (NHS), dicyclohexylcarbodiimide (DCC), hydroxylamine hydrochloride ($\text{H}_2\text{NOH}\cdot\text{HCl}$), *N,N,N*-triethylamine (TEA) were obtained from Aldrich Corporation and used without further purification. Dimethylformamide (DMF), dichloromethane, chloroform, isopropanol and diethyl ether (Shanghai Chemical Reagent Corporation) were purified via distillation with molecular sieves (4 Å). Sulfuric acid (H_2SO_4 , 98%) and chromium trioxide (CrO_3) were purchased from Shanghai Chemical Reagent Corporation and used without further purification. CDCl_3 used as solvents in the NMR measurements was obtained from Aldrich Corporation.

3.2. Synthesis of MPEG active ester [26,27]

MPEG (2.5 g, 0.5 mmol) was dissolved in 25 ml of deionized (DI) water containing 8 ml of H_2SO_4 (95–98%) in a 100 ml round bottom flask; added a solution of CrO_3 (0.33 g, 3.3 mmol, in 5 ml water) to the mixture, and stirred it for 12 h at room temperature. Then 25 ml water was added to the solution and the mixture was stirred for 1 h. To purify the product, we used CH_2Cl_2 (3×100 ml) to extract the PEG-carboxylates and washed the organic layer by water (2×25 ml) and saturated NaCl solution (2×25 ml), successively. After drying with MgSO_4 and concentrating, the organic layer was added to 300 ml diethyl ether. The precipitation was filtered and dried (2.32 g, yield 92.8%). The conversion was over 98% (by the ^1H NMR spectroscopies) and no degradation happened (by GPC).

Afterwards, we dissolved the product (MPEG-COOH, 1.5 g, 0.3 mmol) in 20 ml DMF, and added NHS (0.1725 g, 1.5 mmol) to the solution. Then added DCC (0.3095 g,

1.5 mmol) to the mixture in an ice-water bath, and stirred it under the protection of argon at 0 °C for 1 h and at room temperature for 24 h. The precipitation was removed by filtration. The filtrate was added to diethyl ether (100 ml) and the mixture was cooled by an ice-water bath for 1 h. Finally, the precipitate (MPEG-NHS), a white powder, was obtained after filtering, washing with isopropanol and drying in vacuum at room temperature (1.12 g, yield 74.8%).

3.3. Bonding PEG chains onto AFM tips [27]

The AFM contact tips (purchased from Digital Instrument Company, NP-S) which are made of silicon nitride were washed in chloroform for 11 min and dried in a stream of nitrogen. Then the tips were dipped into piranha solution (30 vol.% H₂O₂/H₂SO₄, 3/7) for half an hour to be cleaned and activated. After being washed with water and chloroform, the tips were dried in a nitrogen stream. We then dipped the tips into the H₂NOH·HCl solution (6.6 g H₂NOH·HCl dissolved in 12 ml DMSO) containing 4 Å molecular sieve beads and kept it at room temperature for 12 h for esterification. Then the tips were washed with DMSO, water and acetone and dried in a nitrogen stream. Subsequently, we dissolved the MPEG active ester (MPEG-NHS, 50 mg, 0.01 mmol) which had been obtained previously in 10 ml CH₂Cl₂ and added TEA (50 μl) into the solution to bond the PEG chain onto the tips. Then the tips modified with –NH₂ were immersed in the solution for 2.5 h. After rinsing in chloroform and drying in nitrogen stream, the tips were kept in DI water.

3.4. Force spectroscopy experiment

As shown in Fig. 2, one PEG chain was anchored on the tip, and the fresh mica was used as substrate. We then moved the piezo tube to approach the substrate to the tip. The repulsive force between the tip (with the chains) and the substrate appeared when the tip contacts the substrate. During this process, PEG chains were adsorbed onto the substrate by physical adsorption and formed bridge structure. The bridge structure was stretched when the tip and substrate departed each other. These interactions resulted in the bending of cantilever against or towards the substrate which was recorded by the detecting system.

The signals of the tip bending and the voltage on the piezo tube were finally transformed to the force spectroscopy.

All force measurements were performed on Multimode-microscope using a Nanoscope IV controller (Digital Instrument, Santa Barbara, CA) with a picoforce accessory which provides high resolution. All force–distance cycles were recorded at 1 Hz vertical scan rate, 60–80 nm *z*-amplitude and 1 nN loading force in the DI water. Further measurements showed the same results at various approaching speeds (at 0.1–10 Hz vertical scan rate) which mean the measurements were performed under thermodynamic equilibrated conditions. The V-shaped Si₃N₄ cantilevers (spring constant range 0.09–0.12 N/m) were used and the constants of the cantilevers were measured by the thermal noise method [28,29]. Totally, 40 tips were modified and 25 tips were chosen to present over 8600 force curves in our experiments.

4. Results and discussion

The SCMFT simulations are performed in cylindrical lattices with 100*b* radius and 200*b* height. The morphology of the chain(s) and the free energy of the system at every distance are obtained and the force curves are calculated from the energy–distance curves by differentiating the free energy with respect to the distances. Many states of the chain(s) on the tip are investigated, for example, different grafted positions, different chain numbers and chain lengths, etc. The experimental results are presented to compare with the simulation results. It should be noted that the simulation in this paper is only suitable for the approaching process, because for a single chain stretching process, the use of the mean field theory to a large extension would cause significant deviation.

4.1. Influence of grafting position

In this section, one end of a Gaussian chain with *N* = 50, is fixed on the tip. The force curves indicating the repulsion and the morphology of the chain when the tip is touching the substrate are shown in Fig. 3. The force curves and the space distribution of the chain segments vary when the chain is grafted at different positions on the tip. To inspect the influence of the grafting position to the approaching force curve, three typical positions were picked out for observing. The three cases are

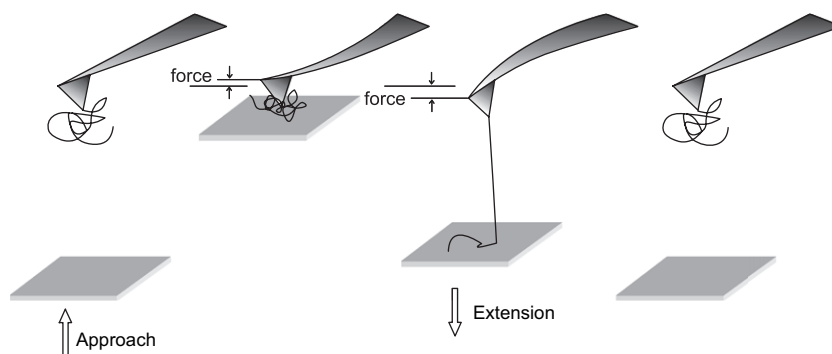


Fig. 2. The sketch picture of the force spectroscopy experiment.

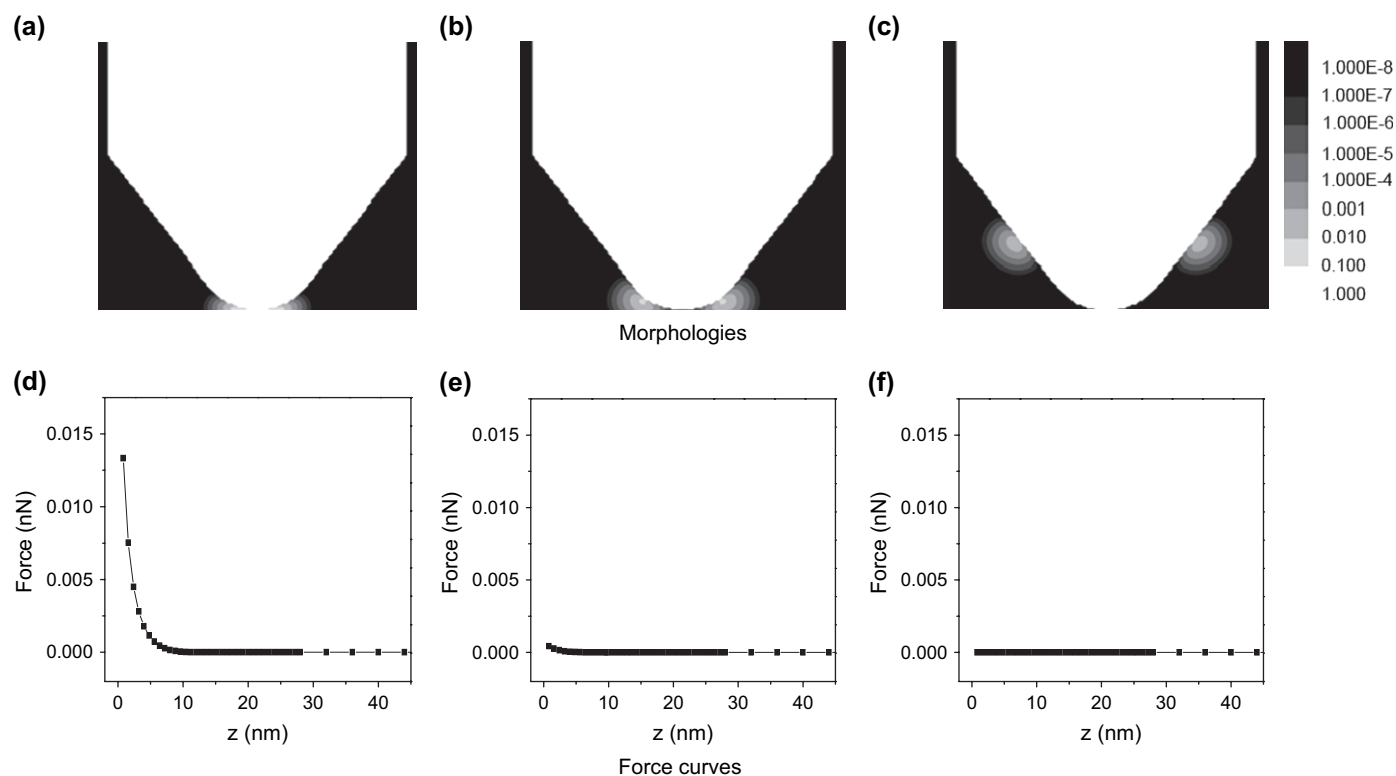


Fig. 3. The distribution of the chain segments (a–c) and the force curves (d–f) when the chain is grafted at different positions of the AFM tip. The chain length is 50 and the chain number is 1; (a) and (d) are the pattern and the force curve of the condition that the chain is grafted on the top center of the tip; (b) and (e) are of the chain grafted slightly departing from the center; (c) and (f) are of the chain grafted far from the center.

proposed based on: (1) the observation of the 8600 force curves of 25 AFM tips grafted with PEG chains; (2) the surface of a cylindrical tip with a cone-like head, possible grafting positions can qualitatively be classified into three different types in terms of the coil size of the polymer chain, which are grafting positions at the top center of the tip, positions deviating from the top center but the distance is at the same order of magnitude of the coil size, and positions far away from the top center (in which the distance is significantly larger than the coil size). Surely, other hybrid situations are also possible because it is difficult to precisely control the number of chains grafted and position where they grafted in the experiment. Such hybrid situation may cause complicated force curves. Since our SCMFT model is a first attempt to simulate the force behavior of the polymer chain grafted AFM tip, we are limited to consider the three relatively clear and neat situations. We expect the results are helpful in the understanding of other more complicated phenomena.

When grafted at the top center of the tip (state (a) shown in Fig. 3), the chain endures a strong extrusion and thus induces an evident repulsion on the force curve, shown in Fig. 3(d). As the grafting point moves away slightly from the top (state (b)), the repulsion falls down to an immeasurable level. However, the chain still has the possibility to touch the substrate in this case. When the chain is grafted to the position far from the top, as is shown in Fig. 3(c), there is no interaction between the chain and the substrate.

Here, we note that there is no adsorption or repulsion between the chain segments and the substrate, which means the repulsion

is only caused by the entropy effect of the polymer chain. For the condition that the chain is grafted on the top center of the tip (state (a) in Fig. 3), it is fixed at the most compressed place, which results in larger repulsion. As the grafting point moves departure (state (b) in Fig. 3) the center, the chain is less compressed at the same tip–substrate distance. Therefore the chain obtains more freedom, resulting in a large drop of the repulsion, even the chain segments still have the possibility to touch the substrate. As the grafting point moves far from the top (state (c) in Fig. 3), the chain segments cannot reach the substrate, there are no interactions between the chain and substrate.

It should be mentioned that for the reason of cylinder symmetry in the simulation, the morphology of the chain appears on both the sides of the tip when the grafting point departs away from the tip center. To ensure the validity of the results, the same calculations have been carried out in a 2D square lattices (200×200), in which the chains only appear on one side of the tip when grafted away from the tip center. With the same parameters and conditions, almost same force curves, except a little difference of the absolute value, have been obtained in these two simulation systems.

4.2. Influence of chain number, chain length, and interaction parameter

In this section, the influence of the chain number, the chain length and the interaction parameter has been investigated

with the simulation in detail. The simulation results are shown in Figs. 4–6.

As expected, for the same tip–segment separation, the repulsion force increases with the increasing of the chain number (shown in Fig. 4). As the chain number is small, for ideal chains the entropy of the system is proportional to the chain number, thus the force should also grow linearly with it. However, in a SCMFT calculation, the excluded volume effect is included through the incompressibility condition, although statistically. Therefore, higher segment concentration leads to more expansion of the chain coils, which results in nonlinear growth of the force with respect to the growth of the chain number. This is demonstrated in the inset of Fig. 4, in which the forces are rescaled by the number of chains grafted on the tip. It is seen that after rescaling by the chain number, at the same tip–substrate distance, the force with more chain number is still higher.

The influence of the chain length on the force curve is shown in Fig. 5. On increasing the chain length, at the same tip–substrate distance the repulsion force increases. This is because confined within the same space, longer chains lose more entropy compared to their free states, since they have more segments that should have realized more configurations if not confined.

Another effect of increasing chain length is that the distance where the repulsion appears becomes larger. In order to observe a repulsion force, the segments of the chain must be able to touch the substrate, however, these segments form a coil attached to the tip since one end is grafted on the tip. Therefore, distance where the repulsion appears is on the order of the magnitude of the coil size, which is $Rg = N^{1/2}b$ for a chain with length N . Indeed, for a grafted chain with $N = 20$ and $b = 0.8$ nm, the coil size is $Rg = 3.5$ nm, coincident with the distance where the repulsion appears (see Fig. 5, the curve with squares). Such estimation is also applicable to other chain lengths.

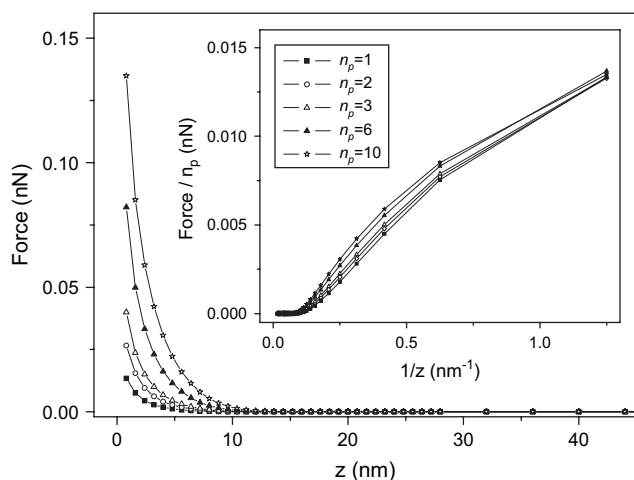


Fig. 4. The force curves for the AFM tip grafted with different number of chains. The chain length used in the simulation is 50. The grafting point is at the top center of the AFM tip. In the inset, the force curves are shown as force vs. inverse of the tip–substrate distance for evidence of the repulsion and the forces are rescaled by the number of chains grafted.

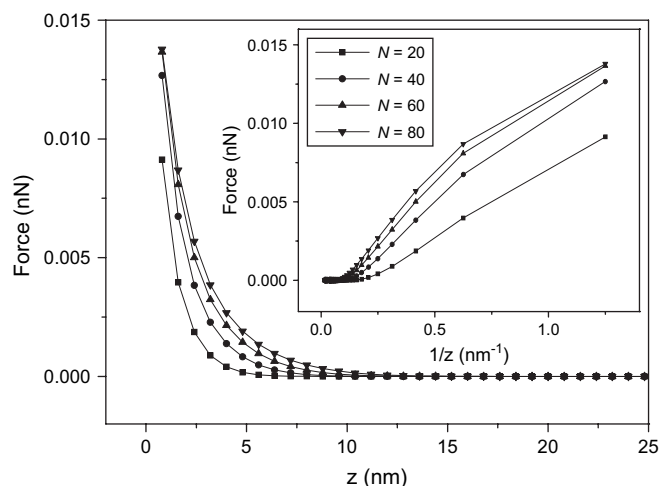


Fig. 5. The force curves for the AFM tip grafted with chains of different lengths. The chain number used in the simulation is 1. The grafting point is at the top center of the AFM tip. In the inset, the force curves are shown as force vs. inverse of the tip–substrate distance for evidence of the repulsion.

Moreover, it is worthy to note that the forces of various chain lengths tend to become closer when the tip is very close to the substrate, i.e., with small tip–substrate distance (as is shown in the inset of Fig. 5). We believe the reason is that under this situation, the chain has been greatly compressed. Therefore, the segments close to the grafted end cannot move out and have been greatly compressed between the tip center and the substrate, which causes the main contribution of the repulsion force. However, the farther segments to the grafted end could be pushed out to the tip side, which results in much less contribution to the repulsion force. Therefore, when the tip is very close to the substrate, the repulsion force is mainly contributed by the segments close to the grafted end, which means that there will be less effect of the chain length when it is beyond a certain value. As the tip moves away from

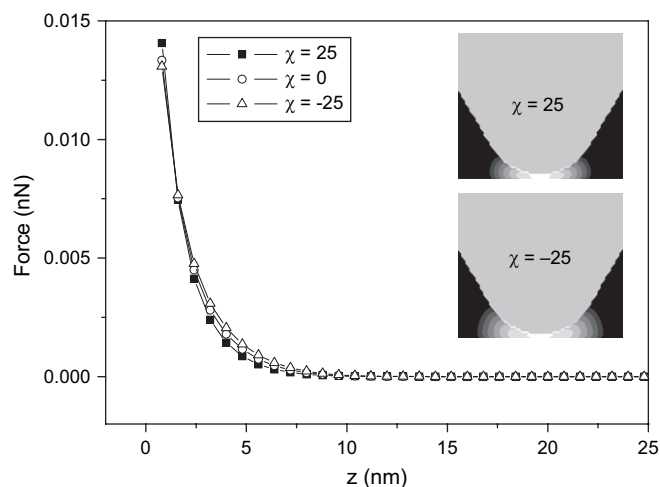


Fig. 6. The force curves for the AFM tip grafted with chains that have different interaction parameters with the solvent. The chain number used in the simulation is 1. The chain length is 50. The grafting point is at the top center of the AFM tip. In the inset, the morphologies of the grafting chain at the separation of 0.8 nm are shown.

the substrate, the contribution of the segments close to the grafted end decreases rapidly and the contribution of the far segments holds the priority. Therefore, the long chain shows higher repulsion than short chain does.

The influence of the interaction parameter χ_{ps} has also been inspected (Fig. 6). As is known, the interaction between the chain segments and the solvent will cause the free energy to decrease when $\chi_{ps} < 0$ and increase when $\chi_{ps} > 0$. Although χ_{ps} causes the morphology of the chain a considerable change, it does not influence the force curve as much. At the same separation distance, increasing the χ_{ps} only causes decrease of the repulsion force, as shown in Fig. 6. This is because the coil size of the chain shrinks with the increase of χ_{ps} , as expected.

4.3. Influence of adsorption between chain segments and substrate

Since adsorption exists between the chain segments and the substrate in real experiment, the influence of the interaction between the chain segments and the substrate has to be discussed. As shown in Fig. 7, the repulsion decreases with the increasing of $|\eta|$ when $\eta < 0$, i.e., strong adsorption of the chain segments reduces the repulsion force. And the force changes from repulsion to attraction when η is about -8 . When $|\eta|$ keeps increasing to a high value, the attraction keeps increasing and a plateau appears when it reaches -15.0 .

When the tip approaches the substrate, the chain(s) on the tip will be pressed and the free energy of the system will increase in the case of no adsorption between the chain segments and the substrate. When there is a weak adsorption, the adsorption will reduce the free energy and make the repulsion less as shown in Fig. 7. As the adsorption become stronger, the adsorption between the chain segments and the substrate turns out to dominate the free energy, and accordingly the force changes to purely

attraction (as shown in Fig. 7 the value of $|\eta|$ is larger than 8.0). However, the adsorption force caused by the interaction between the chain segments and the substrate has seldom been actually measured during the approaching process. We attribute this to the high value of $|\eta|$, because it has exceeded experimental scale when it is over 10.0. When the adsorption strength keeps increasing to a high level ($|\eta| > 15.0$), a plateau appears on the force curve. This is because the chain segments are strongly adsorbed on the substrate and they can only be divorced from the substrate when the chain has been stretched to the length's limit, which is scaled with the separation between the tip and the substrate. Therefore the free energy changes linearly with the separation, and the force appears to be a constant, resulting in a plateau on the force curve.

4.4. Combine with the van der Waals interaction

To make the simulation closer to the real force spectrum, the van der Waals interaction between the tip and the substrate is combined with the simulation results and this shows the drop down of the force when the tip approaches closer to the substrate after the force reaches a peak value. The van der Waals interaction between macroscopic bodies with regular shape can be calculated analytically. For a spherical tip with radius R next to a flat surface the van der Waals potential is given by [30,31]

$$V_{\text{vdW}} = -\frac{A_H R}{6z} \quad (13)$$

Thus the van der Waals force for the tip next to the substrate is thus found to be:

$$f_{\text{vdW}} = -\frac{A_H R}{6z^2} \quad (14)$$

where A_H is the Hamaker constant, which is suggested to be 4.5×10^{-20} J in water, R is set to be $30b$, which is roughly 24 nm, and z is the separation of the center of the closest tip atom from the substrate, equaling to the tip–substrate distance in the simulation. To make the calculated result close to the experiment, we choose the force curve, which is got from the case that 10 chains (with length $N = 50$) are grafted at the top center of the tip, and add it with the van der Waals interaction. The result is shown in Fig. 8.

4.5. Comparison of the simulated and the experimental results

We have also measured the force spectrums of the PEG chains grafted AFM contact tip approaching and stretching processes on the blank mica surface. For many cases of force spectrum measurements, “cleanness” was required which means the chains between tip and substrate are recommended to be very limited. In our experiments, this requirement also existed.

A very efficient esterification was used to chemically bond PEG chains to the tip. The esterification was done in a PEG solution with very low concentration and the interacting

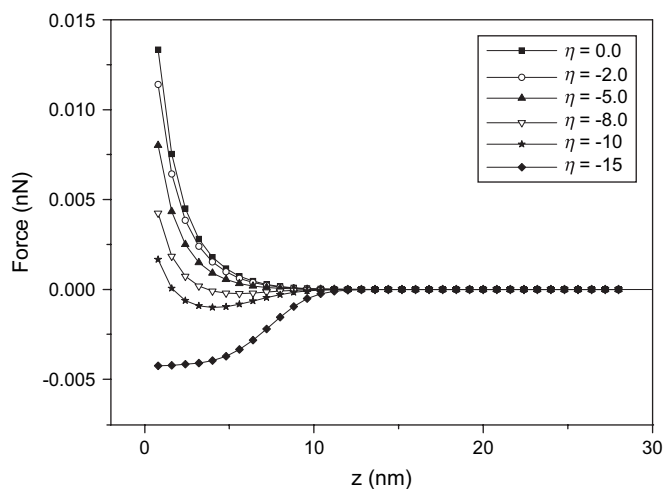


Fig. 7. The force curves for the AFM tip grafted with chains that have different adsorption strengths to the substrate. The chain number used in the simulation is 1 and the chain length is 50. The grafting point is at the top center of the AFM tip. The positive force means repulsion and negative force means attraction.

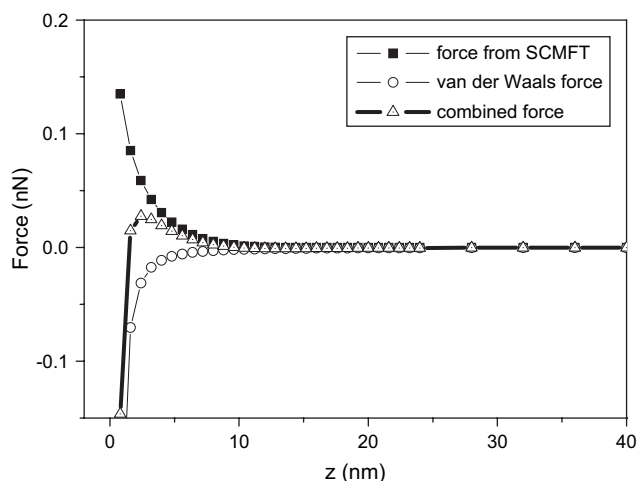


Fig. 8. The simulated force curve combined with van der Waals interaction. The chain number is 10, the chain length is 50 and the grafting point is at the top center of the tip. The van der Waals force curve is calculated by Eq. (14).

time was controlled to be short enough to limit the quantity of the chain grafted. Therefore, there were only a few PEG chains which were able to graft onto the tip. We have modified 40 tips under the same conditions and 25 tips were chosen to do the test and they gave out different force curves. For example, some tips always gave the force curves with repulsion during the approaching process and peaks during the stretching process. However, some tips only gave the force curves when the chains were stretched, no repulsion force was detected as the tip approaches the substrate. The reason that with the same experimental condition different force curves were obtained is explained as follows: the distribution of the PEG chains on the tip is not uniform as a dense layer because of the lack of PEG chains grafted. On the contrary, they grafted randomly onto the tip, in terms of both position and quantity, which resulted in different behaviors.

Based on the behavior of the force curves, the 25 tested tips could be classified into four types qualitatively. The first type exhibits repulsion on the approaching curve and a single stretching peak on the extension curve (Fig. 9(a)). For this situation, it corresponds to the state that the PEG chains have been grafted on the top center of the tip (see Fig. 3(a)). We have drawn a typical simulated force curve in Fig. 9(d), note that for better comparison, a vertical line located at $z = 0$ is added to mimic the dramatic force increase when the tip touches the substrate as observed in the experiment. Since the present form of SCMFT is not applicable to the chain stretching, force curve for the extension process cannot be provided. The second type is shown in Fig. 9(b). There is no repulsion when tip approaches but a single stretching peak is observed on the extension curve. This indicates that no or little extrusion of the chain is present, but the chain can still touch the substrate and adsorb on it, corresponding to the state (b) in Fig. 3, in which the grafting points of the chains deviate from the tip center (with a distance of coil size of

the chains). We also present a force curve corresponding to this situation in Fig. 9(e). The third type is shown in Fig. 9(c), with no repulsion and no stretching peak observed, corresponding to the state that the grafting point is far from the tip top (with distance far larger than the coil size, see Fig. 3(c)) and consequently no touch between the chain and the substrate occurs. A similar simulated force curve is presented in Fig. 9(f).

The force curves of the last type in the experiment shows larger repulsion than that in Fig. 9(a) and multi-peaks occurs, which means that too many chains have been grafted to the tip (figure not shown). For the force spectrum measurement, this state is complex and not recommended and thus it is not discussed in this paper.

Therefore, we can develop a method to inspect the state of the grafted chain on the AFM tip from the simple force spectrum experiment. As has been discussed above, we can qualitatively know the position of the grafting point from the force spectrums. (1) When the approaching force curves of the polymer-grafted tip show a visible repulsion and the stretching force curve only contains a single stretching peak, the polymer chain is grafted on the top center of the tip; (2) When there is no repulsion in the approaching process but a single stretching peak appears on the stretching process, the chain is grafted at the position slightly departing from the top center of the tip (usually within a distance of the coil size). We believe that tips of this type are suitable for many force spectrum experiments such as using PEG as spacer in the antibody–antigen interaction measurement. This is because the chain in this state moves freely without being pressed by the substrate but still has a considerable possibility to reach the substrate; (3) When there is no repulsion and no stretching peak, the chain is grafted at the position far from the top or simply not grafted on the tip; (4) When there are multi-peaks on the force curves, it means too many chains are grafted to the tip.

Finally, we point out that the free energy has a logarithmic relation with the tip–substrate distance, which results in a reciprocal relation between the force and the distance, as shown in Fig. 10. There is a good agreement between the simulation data shown in Fig. 3(a) and the experimental result shown in Fig. 9(a), i.e., when the chain is grafted at the top of the tip, demonstrating the feasibility of our method.

It should be noted that the absolute value of the repulsion force in the simulation is much lower than that in the experiment. We speculate that two reasons are possible: at first, for the sake of simplicity, there was only one chain grafted on the tip in most of the simulations, however, in the experiments there should be multichains grafted on the tip. The discussion on the chain number effect provides us a reasonable explanation. In the cylindrical coordinate, the force increases with the chain number in a linear relation. To reach the experimental force values, at least 10 PEG chains must be grafted on the tip. The second possible reason is that the chains used in simulation are ideal but in experiments they are not soft enough to be regarded as an ideal Gaussian

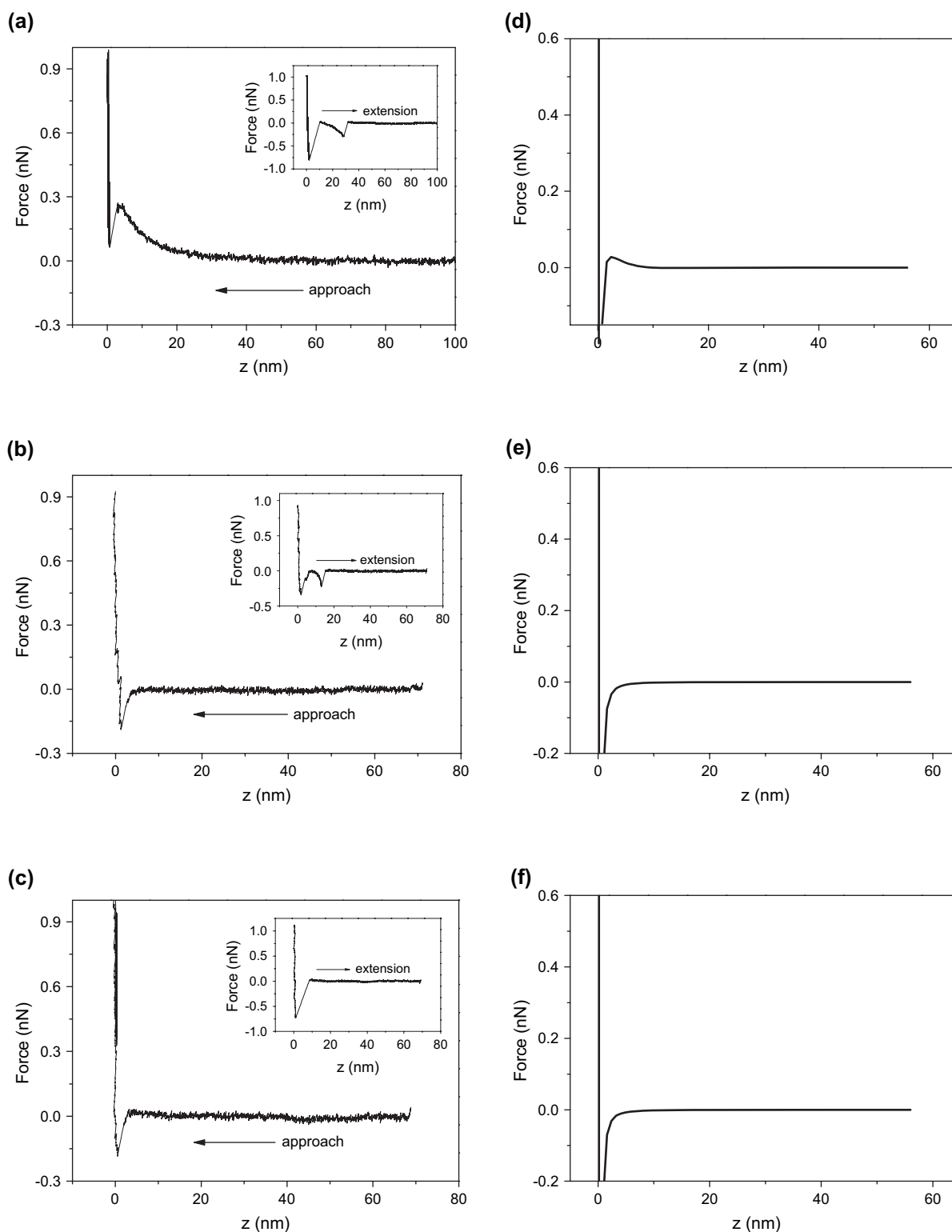


Fig. 9. Comparison of the experimental force curves and the simulated force curves in the approaching process; (a–c) are the experimental force curves; the PEG molecular weight is about 5000 g/mol; (d–f) are the simulated force curves (combined with van der Waals interaction and a vertical line located at $z=0$ to mimic the dramatic force increase when the tip touches the substrate as observed in the experiment), with different grafted positions: at the top of the tip in (d), slightly departing from the center in (e) and far from the center in (f). The chain number is 10 and the chain length is 50. In the insets in (a–c), the force curves measured in the extension process is shown to distinguish which type of grafting position is realized in the chemical binding experiment.

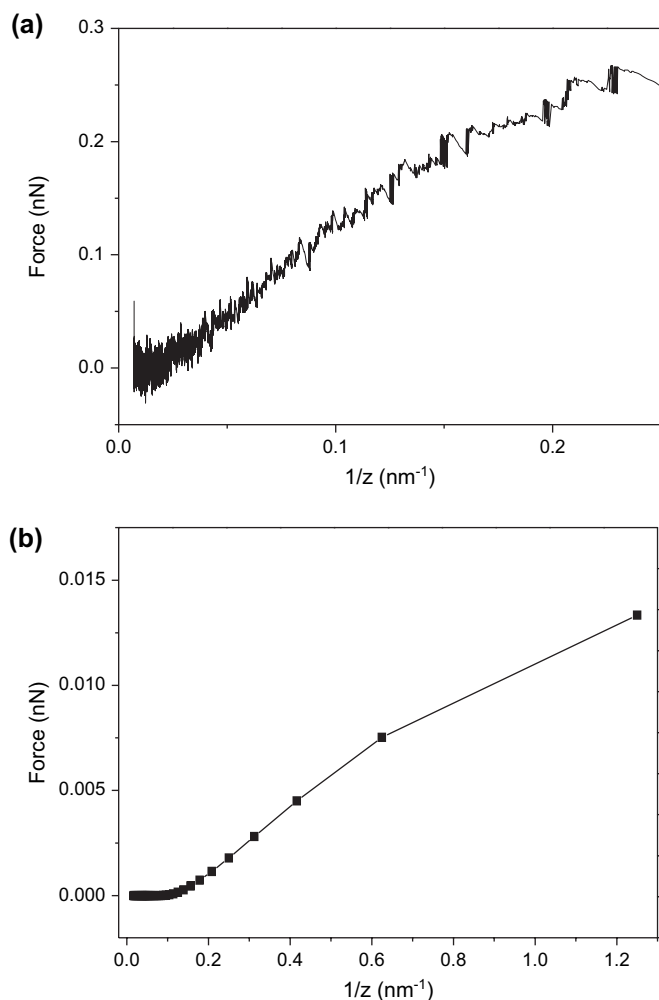


Fig. 10. Comparison of the experimental and the simulation results. Force vs. inverse of tip–substrate distance in the approaching process; (a) is experimental result and (b) is simulation result for the case shown in Fig. 3(a), i.e., the chain grafted at the top of the tip.

chain, further improvement of the chain model beyond Gaussian may need to get more agreement between the simulation and experiment, this, however, is out of the scope of the present paper.

5. Conclusion

A self-consistent mean field theory (SCMFT) model has been developed to describe the force curve of a polymer chain grafted AFM tip as it approaches the substrate. The influences of the grafted position, the grafting chain number, and the chain length have been investigated by simulations based on SCMFT. Experimental results have also been presented, which shows good agreement with the simulation results. Thus we have developed a method to investigate the state of a few chains grafted on the AFM tip by studying the force curves on mica substrate.

Acknowledgement

We gratefully acknowledge financial support from the National Basic Research Program of China (G2005CB6-23800), and the NNSF of China (Grant nos. 20625413 and 20490220).

References

- [1] Egawa H, Furusawa K. *Langmuir* 1999;15:1660.
- [2] Ellis DJ, Shadan S, James PS, Henderson RM, Edwardson JM, Hutchings A, et al. *Journal of Structural Biology* 2002;138:187.
- [3] Fisher MI, Tjarnhage T. *Biosensors and Bioelectronics* 2000;15:463.
- [4] Maeda N, Senden TJ, di Meglio JM. *Biochimica et Biophysica Acta: Biomembranes* 2002;1564:165.
- [5] Christenson EM, Anderson JM, Hiltner A, Baer E. *Polymer* 2005; 46:11744.
- [6] Paige MF. *Polymer* 2003;44:6345.
- [7] Vasilev C, Reiter G, Pispas S, Hadjichristidis N. *Polymer* 2006;47:330.
- [8] Kado S, Yamada K, Kimura K. *Langmuir* 2004;20:3259.
- [9] Grandbois M, Beyer M, Rief M, Clausen-Schaumann H, Gaub HE. *Science* 1999;283:1727.
- [10] Hugel T, Holland NB, Cattani A, Moroder L, Seitz M, Gaub HE. *Science* 2002;296:1103.
- [11] Schönherr H, Beulen MWJ, Bügler J, Huskens J, van Veggel FCJM, Reinhoudt DN, et al. *Journal of the American Chemical Society* 2000;122:4963.
- [12] (a) Rief M, Oesterhelt F, Heymann B, Gaub HE. *Science* 1997;275:1295; (b) Ortiz C, Hadziioannou G. *Macromolecules* 1999;32:780; (c) Cui SX, Liu CJ, Wang ZQ, Zhang X. *Macromolecules* 2004;37:946.
- [13] Hinterdorfer P, Baumgartner W, Gruber HJ, Schilcher K, Schindler H. *Proceedings of the National Academy of Sciences of the United States of America* 1996;93:3477.
- [14] Zhang W, Zhang X. *Progress in Polymer Science* 2003;28:1271.
- [15] (a) Patra M, Linse P. *Nano Letters* 2006;6:133–7; (b) Patra M, Linse P. *Macromolecules* 2006;39:4540.
- [16] Schmid F. *Journal of Physics: Condensed Matter* 1998;10:8105.
- [17] Fredrickson GH, Ganesan V, Drolet F. *Macromolecules* 2002;35:16.
- [18] Matsen MW. *Journal of Physics: Condensed Matter* 2002;14:R21.
- [19] Matsen MW, Schick M. *Physical Review Letters* 1994;72:2660.
- [20] (a) Drolet F, Fredrickson GH. *Physical Review Letters* 1999;83:4317; (b) Bohbot-Raviv Y, Wang ZG. *Physical Review Letters* 2000;85:3428.
- [21] (a) Tyler CA, Morse DC. *Macromolecules* 2003;36:3764; (b) Tyler CA, Morse DC. *Macromolecules* 2003;36:8184.
- [22] Helfand E. *Journal of Chemical Physics* 1975;62:999.
- [23] (a) Hong KM, Noolandi J. *Macromolecules* 1981;14:727–36; (b) Hong KM, Noolandi J. *Macromolecules* 1981;14:736; (c) Hong KM, Noolandi J. *Macromolecules* 1983;16:1083.
- [24] Stasiak A, Dobay A, Dubochet J, Dietler G. *Science* 1999;286:11a.
- [25] Xu JJ, Qiu F, Zhang HD, Yang YL. *Journal of Polymer Science Part B: Polymer Physics* 2006;44:2811.
- [26] Fishman A, Acton A, Lee-Ruff E. *Synthetic Communications* 2004; 34:2309.
- [27] Riener CK, Stroh CM, Ebner A, Klampfl C, Gall AA, Romanin C, et al. *Analytica Chimica Acta* 2003;479:59.
- [28] Florin EL, Rief M, Lehmann H, Ludwig M, Dornmair C, Moy VT, et al. *Biosensors and Bioelectronics* 1995;10:895.
- [29] Butt HJ, Jaschke M. *Nanotechnology* 1995;6:1.
- [30] Giessibl FJ. *Reviews of Modern Physics* 2003;75:949.
- [31] Israelachvili JN. *Intermolecular and surface force*. Academic Press; 1991.